1D lanthanide(III) coordination polymers with disulfide ligand generated *in situ*†‡

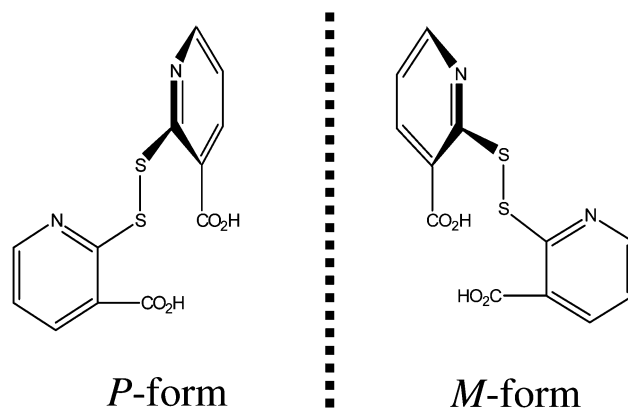Fengyan Li, Lin Xu,* Bo Bi, Xizheng Liu and Lihua Fan

Three 1D Ln(III) - disulfide complexes $[Dy(2,2'-DTDN)_{1.5}(DMSO)_3]\cdot H_2O$ (**1**), $[Nd(2,2'-DTDN)_{1.5}(DMSO)_3]$ (**2**), and $[Eu(2,2'-DTDN)_{1.5}(DMSO)_3]\cdot H_2O$ (**3**) (DTDN = dithiodinicotinate) have been synthesized and characterized with single-crystal X-ray diffraction analysis. The ligand dithiodinicotinate was generated *in situ* by two molecules of 2-mercaptonicotinic acid. These complexes are isostructural except for the lattice water molecules and show a double-chain structure built up from two chiral single-chain motifs. Compound **3** shows strong red fluorescent emissions in the solid state at room temperature. The magnetic properties of these three compounds were studied in the range of 2–300 K.

Introduction

The modular synthesis of metal–organic framework (MOF) structures has received significant attention in the current research to use the coordination preference of metal ions for polydentate ligands. It is well known that the structures of metal–organic architectures are influenced by many factors, such as the coordination nature of the metal ions and ligands, the reaction conditions and so on. For f-block metal ions, they do not show any preference for any particular coordination geometry because the valence orbits are buried inside. Thus, the metal–ligand coordination bonds are mostly ionic, and the nature of the coordination sphere could be controlled by a subtle interplay of metal–ligand interactions, interligand steric constraints and the counteranions. Although the flexibility of the coordination sphere of the f-block metal ions makes design difficult, the pliability together with the tendency towards high coordination numbers makes lanthanide ions attractive for designing new materials with unusual network topologies, and these products can be potentially useful such as luminescent materials,[1] magnetic materials,[2] liquid crystals,[3] radiopharmaceuticals,[4] selective gas absorption,[5] molecular-recognition and chirality-sensing agents in biology,[6] MRI contrast agents[7] and so on.

Recently, many examples of lanthanide-based frameworks with multi-dentate organic ligands such as sulfoxides,[8] carboxylates,[9] pyridones and lactams[10,11] have been established by single-crystal X-ray analyses. However, the lanthanide networks using disulfide derivatives of carboxylates as ligands are still unexplored. The disulfide derivative of the nicotinate, dithiodinicotinate (DTDN), adopts a twisted structure and C–S–S–C

torsion angle of *ca.* 90° in the solid state, which shows the axial chirality with the *M*- and *P*-forms of the enantiomers (Scheme 1). In particular, such disulfide derivatives can act as the organic bridging "spacer" to create interesting topology structures with chiral structural motifs when combined with lanthanide ions. Searching for the related literature shows that aromatic and aliphatic thiolates can be oxidized to disulfide complexes under suitable conditions.[12] Hence we selected the multidentate and multifunctional ligand 2-mercaptonicotinic acid (2-MNA) to design and synthesize new lanthanide coordination polymers with ligands generated *in situ*. In this work, we successfully obtained three new lanthanide disulfide coordination polymers $[Dy(2,2'-DTDN)_{1.5}(DMSO)_3]\cdot H_2O$ (**1**), $[Nd(2,2'-DTDN)_{1.5}(DMSO)_3]$ (**2**) and $[Eu(2,2'-DTDN)_{1.5}(DMSO)_3]\cdot H_2O$ (**3**), which all have a double-chain structure comprised of two chiral single-chain motifs. In addition, the photoluminescence spectrum of compound **3** shows an intense red luminescence at room temperature in the solid state and the magnetic properties of these three compounds were studied in the range of 2–300 K.

Key Laboratory of Polyoxometalates Science, Ministry of Education, College of Chemistry, Northeast Normal University, Changchun, 130024, P. R. China. E-mail: linxu@nenu.edu.cn

Scheme 1 The enantiomers of dithiodinicotinate (DTDN) showing axial chirality.

Experimental

Materials and methods

All chemicals purchased were of reagent grade and used without further purification. Elemental analyses (C, H and N) were performed on a Perkin-Elmer 2400 Elemental Analyzer. The IR spectra were obtained in the range 400–4000 cm^{-1} on the Alpha centaure FT-IR spectrophotometer using KBr pellets. The luminescence spectra were recorded on a Hitachi F-4500 fluorescence spectrophotometer. The magnetic susceptibility measurements for **1**, **2** and **3** were carried out on polycrystalline samples using a Quantum Design MPMS-XL-5 SQUID magnetometer in the temperature range 2–300 K and magnetic field up to 5 T. Diamagnetic corrections were estimated from Pascal's constants.

Synthesis of complexes

0.05 g 2-mercaptonicotinic acid (0.33 mmol) was dissolved in 20 ml DMSO and then 0.1 ml triethylamine was dropped in with stirring. After 5 min, $LnCl_3 \cdot 6H_2O$ (0.53 mmol) was added to the solution. The mixture was stirred continuously at room temperature for about two hours, and then filtered. The filtrate was kept in room temperature for about three months to form yellow crystals. Crystals of **1–3** are stable in the air and insoluble in most common polar and nonpolar solvents once isolated. Yield: 70% for **1**, 40% for **2** and 66% for **3**.

Anal. calcd for $C_{24}H_{29}N_3S_6DyO_{10}$ (**1**): C, 32.94; H, 3.32; N, 4.80%. Found: C, 33.72; H, 3.61; N, 4.76%. IR (cm^{-1}, KBr): 3487 m, 3417 m, 1580 s, 1538 m, 1446 m, 1408 s, 1369 s, 1228 w, 1160 w, 1110 w, 1070 m, 1000 s, 962 s, 856 m, 764 m, 737 m, 650 w, 563 w.

Anal. calcd for $C_{24}H_{27}N_3S_6NdO_9$ (**2**): C, 34.36; H, 3.22; N, 5.01%. Found: C, 34.22; H, 3.54; N, 5.12%. IR (cm^{-1}, KBr): 1580 s, 1536 s, 1448 m, 1400 s, 1370 s, 1235 w, 1159 w, 1115 w, 1067 m, 1018 m, 958 s, 852 s, 764 s, 735 s, 647 w, 547 w.

Anal. calcd for $C_{24}H_{29}N_3S_6EuO_{10}$ (**3**): C, 33.34; H, 3.36; N, 4.86%. Found: C, 33.42; H, 3.24; N, 4.93%. IR (cm^{-1}, KBr): 3490 m, 3418 m, 1590 s, 1530 m, 1450 w, 1408 s, 1370 s, 1230 w, 1160 w, 1110 w, 1020 s, 953 s, 858 m, 762 m, 735 m, 650 w, 563 w.

X-Ray crystallography†

Crystal data and details of data collections and refinements for the structures reported are summarized in Table 1. All measurements were made on a Rigaku R-AXIS RAPID IP diffractometer at 293 K using graphite-monochromated Mo Kα radiation ($\lambda = 0.71073$Å) and oscillation scans technique in the range of $3.01 < \theta < 27.48°$ for **1**, $3.13 < \theta < 27.49°$ for **2** and $1.72 < \theta < 28.29°$ for **3**. Block single crystals of **1** ($0.30 \times 0.10 \times 0.10$ mm), of **2** ($0.30 \times 0.15 \times 0.10$ mm) and of **3** ($0.30 \times 0.10 \times 0.05$ mm) were mounted on the end of a glass fiber capillary. Empirical absorption correction was applied. The structure was solved by direct methods using the program SHELXS-97 and refined by full-matrix least-squares methods on F^2 using the SHELXL-97 program package.[13] All the non-hydrogen atoms were refined anisotropically. In complex **2**, S1 and C22 are disordered over two positions with an occupation of 50% each. Crystal data for **1**, **2** and **3** are summarized in Table 1. Selected bond lengths and angles are given in Table 2. CCDC reference numbers are 642851–642853.†

Results and discussion

Preparation of compounds

The successful isolation of the title compounds depends on the following two aspects: (1) *in situ* oxidation of the ligand to form disulfides, (2) the solvent used in the system. When using water as the solvent, the reaction of Ln ions with only the ligand gives colorless crystals which can be characterized with X-ray diffraction analysis, revealing that the complex was the

Table 1 Crystal data and structure refinement

	1	2	3
Empirical formula	$C_{24}H_{29}DyN_3O_{10}S_6$	$C_{24}H_{27}NdN_3O_9S_6$	$C_{24}H_{29}EuN_3O_{10}S_6$
Formula weight	874.36	838.09	863.82
T/ K	293(2)	293(2)	293(2)
λ/Å	0.71073	0.71073	0.71073
Space group	$P\bar{1}$	$P\bar{1}$	$P\bar{1}$
Crystal system	Triclinic	Triclinic	Triclinic
a/Å	7.8528(16)	7.7400(15)	7.8341(3)
b/Å	11.780(2)	12.154(2)	11.8843(5)
c/Å	17.456(4)	17.433(4)	17.5342(8)
α/°	93.85 (3)	73.85(3)	94.087(10)
β/°	94.70(3)	88.22(3)	94.699(10)
γ/°	91.87(3)	88.55(3)	91.995(10)
V/Å³	1604.5(6)	1574.2(5)	1621.50(12)
Z, D_{calc}/g cm⁻³	2, 1.810	2, 1.768	2, 1.769
μ/mm⁻¹	2.776	2.101	2.377
Reflections collected	15660	15379	10161
Unique reflections	7181	7042	7454
	[R(int) = 0.0269]	[R(int) = 0.0817]	[R(int) = 0.0366]
Goodness-of-fit on F^2	1.221	0.988	1.015
$R1$[a] / $wR2$[b] [$I > 2\sigma(I)$]	0.0266 / 0.0698	0.0541 / 0.1142	0.0499 / 0.0878
$R1$[a] / $wR2$[b] (all data)	0.0307 / 0.0707	0.0752 / 0.1264	0.0779 / 0.1085

[a] $R1 = \sum ||F_o| - |F_c||/\sum|F_o|$. [b] $wR2 = \sum[w(F_o^2 - F_c^2)^2]/\sum[w(F_o^2)^2]^{1/2}$

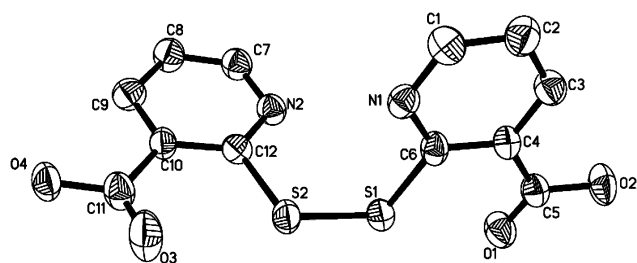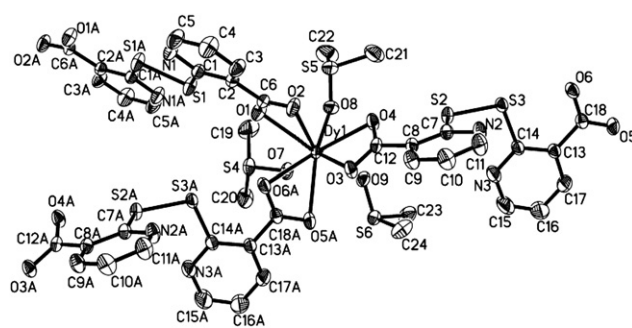**Table 2** Selected bond lengths (Å) and angles (°) for compounds **1**, **2** and **3** [a]

1		2		3	
Dy(1)–O(9)	2.340(2)	Nd(1)–O(9)	2.401(4)	Eu(1)–O(7)	2.359(4)
Dy(1)–O(8)	2.353(3)	Nd(1)–O(5)	2.427(4)	Eu(1)–O(9)	2.388(4)
Dy(1)–O(7)	2.370(2)	Nd(1)–O(6)	2.466(5)	Eu(1)–O(8)	2.391(4)
Dy(1)–O(2)	2.396(3)	Nd(1)–O(1)	2.484(4)	Eu(1)–O(1)	2.426(5)
Dy(1)–O(6)#1	2.409(2)	Nd(1)–O(4)	2.495(4)	Eu(1)–O(4)#1	2.459(4)
Dy(1)–O(3)	2.432(2)	Nd(1)–O(8)#1	2.518(5)	Eu(1)–O(5)	2.452(4)
Dy(1)–O(4)	2.488(2)	Nd(1)–O(3)	2.574(4)	Eu(1)–O(6)	2.529(4)
Dy(1)–O(5)#1	2.529(3)	Nd(1)–O(7)#1	2.574(5)	Eu(1)–O(3)#1	2.555(5)
Dy(1)–O(1)	2.591(3)	Nd(1)–O(2)	2.607(4)	Eu(1)–O(2)	2.598(4)
O(2)–Dy(1)–O(1)	52.22(8)	O(9)–Nd(1)–O(5)	78.40(16)	O(7)–Eu(1)–O(9)	79.17(15)
O(3)–Dy(1)–O(1)	127.94(9)	O(9)–Nd(1)–O(6)	77.32(16)	O(7)–Eu(1)–O(8)	80.58(15)
O(7)–Dy(1)–O(2)	126.57(9)	O(5)–Nd(1)–O(6)	85.59(15)	O(9)–Eu(1)–O(8)	78.74(15)
O(7)–Dy(1)–O(4)	144.89(9)	O(9)–Nd(1)–O(1)	129.95(15)	O(7)–Eu(1)–O(1)	150.43(15)
O(8)–Dy(1)–O(1)	74.87(9)	O(5)–Nd(1)–O(1)	85.84(15)	O(9)–Eu(1)–O(1)	92.38(16)
O(8)–Dy(1)–O(4)	73.94(9)	O(6)–Nd(1)–O(1)	148.65(16)	O(8)–Eu(1)–O(1)	125.87(14)
O(9)–Dy(1)–O(8)	78.81(9)	O(9)–Nd(1)–O(4)	150.00(15)	O(7)–Eu(1)–O(5)	83.80(15)
O(9)–Dy(1)–O(2)	150.32(9)	O(5)–Nd(1)–O(4)	123.26(15)	O(9)–Eu(1)–O(5)	125.88(14)

[a] Symmetry transformations used to generate equivalent atoms: #1 x, $y + 1$, z.
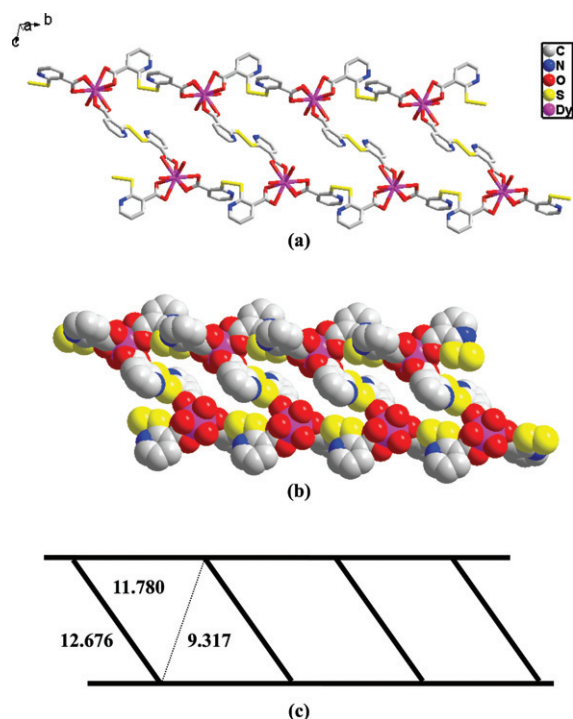
dithiodinicotinate (DTDN, as shown in Fig. 1), coming from the oxidation of MNA under aerobic conditions. A similar phenomenon was also found in recent studies.[14,15] Taking into account the small solubility of DTDN in water, the organic solvent DMSO was used instead. In DMSO, the ligand MNA can also be oxidized to DTDN and, what is more, the DTDN can further react with the Ln ions, forming the double chain structure of lanthanide disulfide complexes.

Crystal structures of [Dy(2,2′-DTDN)$_{1.5}$(DMSO)$_3$]·H$_2$O (1), [Nd(2,2′-DTDN)$_{1.5}$(DMSO)$_3$] (2) and [Eu(2,2′-DTDN)$_{1.5}$(DMSO)$_3$]·H$_2$O (3)

The structure analysis by X-ray diffraction reveals that compounds **1**–**3** are isomorphous, except for the lattice water molecules, and crystallize in triclinic system, space group P-1. Here complex **1** is discussed in detail. Each asymmetric unit contains one dysprosium(III) ion, one and a half DTDN ligands, three coordinated DMSO molecules, and one free guest water molecule. The perspective view of **1** together with the atomic numbering scheme is illustrated in Fig. 2. As shown in Fig. 2, the Dy^{3+} ion is nine-coordinated by six oxygen atoms of the carboxylate groups from three different DTDN^{2-} ligands and three oxygen atoms from three coordinated DMSO molecules in tricapped trigonal prism geometry. The Dy–O distances range from 2.340(2) to 2.591(3) Å. The average Dy–O distance is


Fig. 2 ORTEP representation of the asymmetric unit of complex **1** and associated symmetry-equivalent atoms drawn at the 30% probability level. Hydrogen atoms were omitted for clarity.

2.434 Å, which is close to that of the reported average Ln–O values of 2.448 Å in similar DyO$_9$ environments. It should be noted that the DTDN ligands can be described as two types (I and II) in the ratio 1 : 2. In type I, the dihedral angle between aromatic groups due to disulfide bridging is 0° (C1–S1–S1A–C1A), hence the adjacent rings are coplanar; in type II, the dihedral angle in the adjoining disulfide bridges is 89.3° (C7–S2–S3–C14), so adjacent rings are close to perpendicular. The DTDN ligand of type I adopts a chelation mode linking two dysprosium ions along the [010] direction serving as the "up-right" of the ladder, and the DTDN of type II connects the two dysprosium ions of neighboring edges acting as the "step" of the ladder, also in a chelation mode. The ladder is different from those commonly encountered, the rungs of which are not perpendicular to the edges but close to 60°. The ladderlike double chain extends in a zigzag form, with Dy⋯Dy separations of 9.317, 11.780 and 12.676 Å respectively (as shown in Fig. 3). Compared with the lanthanide 2,2′-bipyridine-4,4′-bicarboxylate coordination polymers,[9h] the Ln⋯Ln distance is much longer because of the DTDN bridging "spacer". In addition, the double chains are further linked by hydrogen bonding (O3⋯O1w: 2.830, O7⋯O1w: 2.919, O1w⋯S6: 3.245 Å) to generate a three-dimensional network structure.

Fig. 1 The structure of the ligand H$_2$DTDN·H$_2$O (the free water molecule and the hydrogen atoms were omitted for clarity).

Fig. 3 (a) View of the 1D ladderlike double-chain structure of complex **1** with type II ligand DTDN (see text) as the rungs. (b) Spacefilling view of the ladderlike double chain. (c) Schematic illustration of the ladderlike double chain.

An interesting aspect of the structure is that if we cut the double chain into two halves each single chain acts as a chiral structural motif, which comprises alternate linking of Dy^{3+} and one of either the *M*- or the *P*-form of the DTDN ligands, as shown in Fig. 4. However, the centrosymmetric space group (*P*-1) leads to an achiral double chain structure in the solid state.
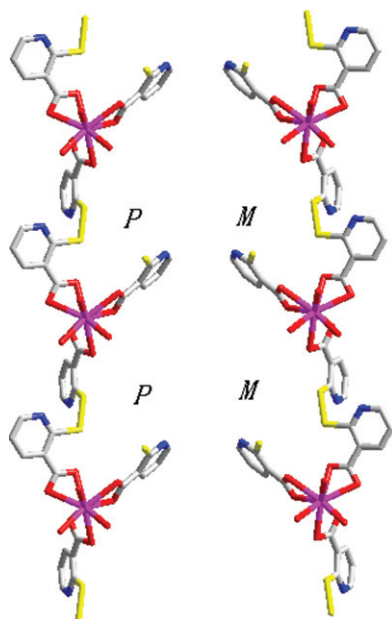
Fig. 4 The chiral single-chain structure linking by only the *M*- or the *P*-form of the DTDN ligands, left (—*P*—*P*—*P*—) and right (—*M*—*M*—*M*—).
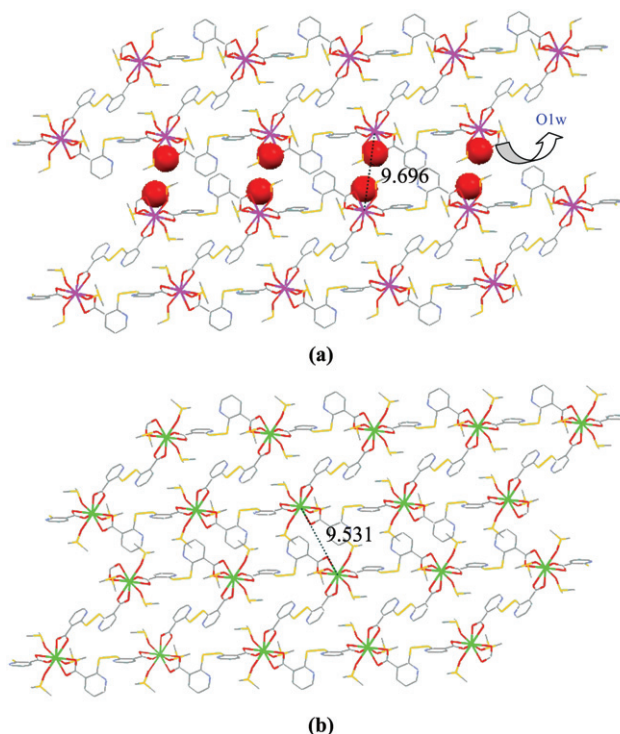
Fig. 5 (a) Packing of the double chains of complex **1** in the *bc* plane. The lattice water molecules are in the spacefill form and in red, which separate the double chains. (b) Packing of the double chains of complex **2** in the *bc* plane, showing shorter distance between different chains than complex **1**.

Compared with compound **1**, the ladder chains in complex **2** stack compactly without any lattice water molecule residing inside, which corresponds to the smaller cell volume 1574.2 Å³ (1604.5 Å³ for **1**). The nearest distance between the neighboring Nd^{3+} ions in different double chains is 9.531 Å, which is also shorter than that in compound **1** (9.696 Å) (as shown in Fig. 5).

IR spectrum and photoluminescence properties

The infra-red spectra of compounds **1** and **3** show a sharp peak around 3420 cm^{-1} due to the O–H stretch of the water molecules but no peak appears in this region in compound **2**, which is also in accord with the results of the single-crystal X-ray analyses.

The photoluminescence spectra for powder samples of compounds **1**–**3** were measured at room temperature, but only compound **3** shows an intense luminescence property. As shown in Fig. 6, the photoluminescence spectrum of compound **3** displays intense red luminescence and exhibits the characteristic transition of $^5D_0 \rightarrow {}^7F_J$ ($J = 0$–4) of the Eu^{3+} ion. The peaks at 579, 592, 616, 650 and 698 nm are attributed to the $^5D_0 \rightarrow {}^7F_0$, $^5D_0 \rightarrow {}^7F_1$, $^5D_0 \rightarrow {}^7F_2$, $^5D_0 \rightarrow {}^7F_3$ and $^5D_0 \rightarrow {}^7F_4$ transitions respectively. The observation of the symmetry-forbidden emission $^5D_0 \rightarrow {}^7F_0$ reveals that Eu^{3+} in **3** occupies sites with low symmetry and without an inversion center. The intensity of the $^5D_0 \rightarrow {}^7F_2$ transition is extremely sensitive to chemical bonds in the vicinity of Eu^{3+}, which increases as the site symmetry of Eu^{3+} center decreases; while the intensity of the $^5D_0 \rightarrow {}^7F_1$ transition depends only slightly on the nature of the environment of the Eu^{3+} center. Therefore, the $I(^5D_0 \rightarrow {}^7F_2) : I(^5D_0 \rightarrow {}^7F_1)$ ratio
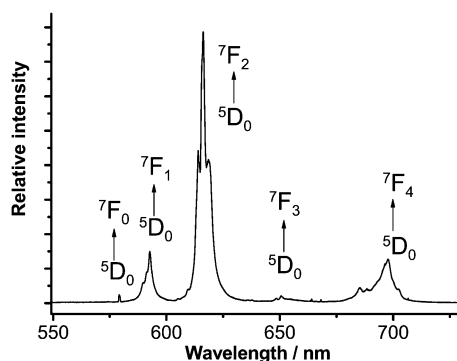
Fig. 6 Emission spectra of compound **3** in the solid state at room temperature (excitation at 488 nm).

is widely used to measure the coordination state and site symmetry of the lanthanide ions.[16] The intensity ratio $I(^5D_0 \rightarrow {}^7F_2) : I(^5D_0 \rightarrow {}^7F_1)$ for compound **3** is about 5.5, which also indicates the low site symmetry of the Eu^{3+} ion in **3**.

Magnetic properties

The temperature dependence of magnetic susceptibility χ_m for compounds **1**, **2** and **3** was investigated in the range 2–300 K with an applied field of 1000 Oe. As shown in Fig. 7, upon cooling of the sample, the χ_m value of compound **1** increases, reaching a maximum of 2.17 emu mol^{-1} at 4.0 K, and then decreases on further cooling. The $\chi_m T$ value stays basically at 13.37 emu K mol^{-1} from room temperature down to about 50 K, close to the expected value of 14.17 emu K mol^{-1} for one non-interacting Dy(III) center ($J = 15/2$ and $g = 4/3$) with a $^6H_{15/2}$ ground state, then suddenly drops down to 3.15 emu K mol^{-1} at 2 K. The best linear fit according to the Curie–Weiss law in the range of 10–300 K yields $C = 13.70$ emu K mol^{-1} and $\theta = -6.92$ K (see Fig. S1‡). The sharp drop of $\chi_m T$ at low temperature as well as a negative θ value is mainly attributed to the ligand field split of Dy^{3+} ion due to a strong spin–orbital coupling together with a weak antiferromagnetic interaction between the neighboring Dy ions.

To confirm this, we also plot the variation of the magnetization with magnetic field at 2 K as shown in Fig. S2.‡ The molar magnetization increases with the increase of the field, indicating that the excited spin states are significantly populated at such
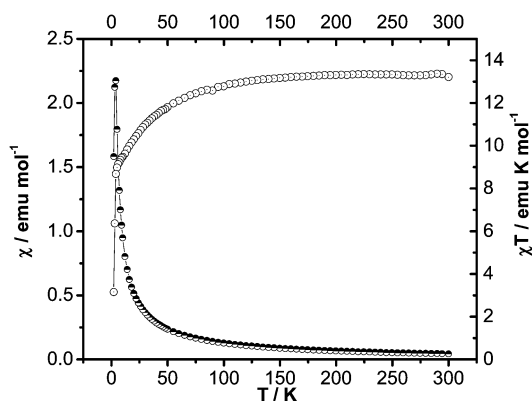
a low temperature. And independent Brillouin functions, with $J = 15/2$ and $g = 4/3$ are plotted. As can be seen, the $M(H)$ curve is deviated from the simulation line with a spin moment less than a single Dy^{3+} ion ($J = 15/2$). Such a partial polarization is due to very weak antiferromagnetic couplings between the magnetic centers.

The $\chi_m T$ vs. T curve of compound **2** is shown in Fig. S3.‡ The $\chi_m T$ value at room temperature is determined to be 1.35 emu K mol^{-1}, which is close to the theoretical value of 1.64 emu K mol^{-1} for the free Nd^{3+} ion.[17] As can be seen from Fig. S3,‡ the $\chi_m T$ value decreases continuously to a value of 0.481 emu K mol^{-1} at 2.0 K. The thermal variation of $\chi_m T$ mainly depends on the populations of the Stark levels arising from the crystal-field perturbation and on the possible antiferromagnetic interactions between the two Nd(III) ions. As for complex **3**, the $\chi_m T$ value continuously decreases and tends to a value very close to zero as the temperature approaches absolute zero (see Fig. S4 in ESI‡), owing to the depopulation of the Stark levels for a single Eu^{3+} ion, which indicates a $J = 0$ ground state for the Eu^{3+} ion ($^7F_0$) at the lowest temperature.

Conclusions

Three new lanthanide disulfide coordination polymers [Ln(2,2'-DTDN)$_{1.5}$(DMSO)$_3$]·nH$_2$O (Ln = Dy, Nd and Eu) have been synthesized and structurally characterized through X-ray diffraction analysis revealing a 1D double-chain structure of Ln(III) ions and DTDN ligands with chiral structural motifs, which proved that by means of adopting the twisted, flexible bridging ligand, it is possible to assemble lanthanide MOFs with new topology structures. We believe that pure chiral crystals will be obtained through controlling the coordination modes of the lanthanide ions; further studies are still in progress.

References

1 N. Sabbatini, M. Guardigli and J. M. Lehn, *Coord. Chem. Rev.*, 1993, **123**, 201.
2 (*a*) T. Sanada, T. Suzuki, T. Yoshida and S. Kaizaki, *Inorg. Chem.*, 1998, **37**, 4712; (*b*) S. Decurtins, M. Gross, H. W. Schmalle and S. Ferlay, *Inorg. Chem.*, 1998, **37**, 2443; (*c*) J. P. Costes, A. Dupuis and J. P. Laurent, *J. Chem. Soc., Dalton Trans.*, 1998, 735; (*d*) R. E. P. Winpenny, *Chem. Soc. Rev.*, 1998, **27**, 447; (*e*) J. P. Costes, F. Dahan, A. Dupuis and J. P. Laurent, *Inorg. Chem.*, 1997, **36**, 3429; (*f*) I. Ramade, O. Kahn, Y. Jeannin and F. Robert, *Inorg. Chem.*, 1997, **36**, 930; (*g*) J. L. Sanz, R. Ruiz, A. Gleizes, F. Lloret, J. Faus, M. Julve, J. J. Borra's- Almenar and Y. Journaux, *Inorg. Chem.*, 1996, **35**, 7384; (*h*) C. Benelli, A. Caneschi, D. Gatteschi and R. Sessoli, *J. Appl. Phys.*, 1993, **73**, 5333; (*i*) C. Benelli, A. Caneschi, D. Gatteschi and R. Sessoli, *Inorg. Chem.*, 1993, **32**, 4797; (*j*) C. Benelli, A. Caneschi, D. Gatteschi, L. Pardi and P. Rey, *Inorg. Chem.*, 1990, **29**, 4223; (*k*) C. Benelli, A. Caneschi, D. Gatteschi, L. Pardi, P. Rey, D. P. Shum and R. L. Carlin, *Inorg. Chem.*, 1989, **28**, 272; (*l*) C. Benelli, A. Caneschi, D. Gatteschi, L. Pardi and P. Rey, *Inorg. Chem.*, 1989, **28**, 275; (*m*) A. Setyiawati, S. Liu, S. J. Rettig, R. C. Thomson and C. Orvig, *Inorg. Chem.*, 2000, **39**, 496.

Fig. 7 Plots of χ_m and $\chi_m T$ vs. T for a polycrystalline sample of complex **1**.

3 K. Binnemans and C. Gorller-Walrand, *Chem. Rev.*, 2002, **102**, 2303.
4 V. W. W. Yam and K. K. W. Lo, *Coord. Chem. Rev.*, 1999, **184**, 157.
5 L. Pan, K. M. Adams, H. E. Hernandez, X. Wang, C. Zheng, Y. Hattori and K. Kaneko, *J. Am. Chem. Soc.*, 2003, **125**, 3062.
6 H. Tsukube and S. Shinoda, *Chem. Rev.*, 2002, **102**, 2389.
7 (*a*) R. B. Lauffer, *Chem. Rev.*, 1987, **87**, 901; (*b*) S. Aime, M. Botta, M. Fasano and E. Terreno, *Chem. Soc. Rev.*, 1998, **27**, 19; (*c*) P. Caravan, J. J. Ellison, T. J. McMurry and R. B. Lauffer, *Chem. Rev.*, 1999, **99**, 2293; (*d*) C. T. W. Moonen, P. C. M. van Zijl, J. A. Frank, D. Le Bihan and E. D. Becker, *Science*, 1990, **250**, 53; (*e*) K. Kumar, C. A. Chang and M. F. Tweedle, *Inorg. Chem.*, 1993, **32**, 587; (*f*) K. Micskei, D. H. Powell, L. Helm, E. Brucher and A. E. Merbach, *Magn. Reson. Chem.*, 1993, **31**, 1011; (*g*) G. Gonzalez, D. H. Powell, V. Tissieres and A. E. Merbach, *J. Phys. Chem.*, 1994, **98**, 53; (*h*) D. H. Powell, O. M. Ni Dhubhghaill, D. Pubanz, L. Helm, Y. S. Lebedev, W. Schlaepfer and A. E. Merbach, *J. Am. Chem. Soc.*, 1996, **118**, 9333; (*i*) S. Aime, M. Botta, S. G. Crich, G. B. Giovenzana, G. Jommi, R. Pagliarin and M. Sisti, *Inorg. Chem.*, 1997, **36**, 2992.
8 R. H. Zhang, B. Q. Ma, X. H. Bu, H. G. Wang and X. K. Yao, *Polyhedron*, 1997, **16**, 1123.
9 (*a*) T. M. Reineke, M. Eddaoudi, D. Moler, M. O'Keeffe and O. M. Yaghi, *J. Am. Chem. Soc.*, 2000, **122**, 4843; (*b*) E. Lee, J. Heo and K. Kim, *Angew. Chem., Int. Ed.*, 2000, **39**, 2699; (*c*) J. G. Mao, H. J. Zhang, J. Z. Ni, S. B. Wang and T. C. W. Mak, *Polyhedron*, 1999, **18**, 1519; (*d*) L. Ma, O. R. Evans, B. M. Foxman and W. Lin, *Inorg. Chem.*, 1999, **38**, 5837; (*e*) L. Pan, X. Huang, J. Li, Y. Wu and N. Zheng, *Angew. Chem., Int. Ed.*, 2000, **39**, 527; (*f*) T. M. Reineke, M. Eddaoudi, M. O'Keeffe and O. M. Yaghi, *Angew. Chem., Int. Ed.*, 1999, **38**, 2590; (*g*) T. M. Reineke, M. Eddaoudi, M. Fehr, D. Kelley and O. M. Yaghi, *J. Am. Chem. Soc.*, 1999, **121**, 1651; (*h*) J. Y. Wu, T. T. Yeh, Y. S. Wen, J. Twu and K. L. Lu, *Cryst. Growth Des.*, 2006, **6**, 467.
10 (*a*) D. M. L. Goodgame, S. Menzer, A. M. Smith and D. J. Williams, *Chem. Commun.*, 1997, 339; (*b*) D. M. L. Goodgame, S. P. W. Hill and D. J. Williams, *Inorg. Chim. Acta*, 1998, **272**, 131.
11 (*a*) G. A. Doyle, D. M. L. Goodgame, S. P. W. Hill and D. J. Williams, *J. Chem. Soc., Chem. Commun.*, 1993, 207; (*b*) L. H. Carrad, D. M. L. Goodgame, S. P. W. Hill and D. J. Williams, *J. Chem. Soc., Dalton Trans.*, 1993, 1003; (*c*) D. M. L. Goodgame, S. Menzer, A. T. Ross and D. J. Williams, *Inorg. Chim. Acta*, 1996, **251**, 141.
12 (*a*) A. G. Lappin and A. McAuley, *J. Chem. Soc., Dalton Trans.*, 1978, 1606; (*b*) D. Cavallini, C. DeMarco, S. Dupre and G. Rotilio, *Arch. Biochem. Biophys.*, 1969, **130**, 354; (*c*) R. Holwerda, *J. Inorg. Biochem.*, 1988, **33**, 131.
13 (*a*) G. M. Sheldrick, *SHELXS-97, Program for solution of crystal structures*, University of Göttingen, Germany, 1997; (*b*) G. M. Sheldrick, *SHELXL-97, Program for refinement of crystal structures*, University of Göttingen, Germany, 1997.
14 S. M. Humphrey, R. A. Mole, J. M. Rawson and P. T. Wood, *Dalton Trans.*, 2004, 1670.
15 J. X. Zhu, Y. J. Zhao, M. C. Hong, D. F. Sun, Q. Shi and R. Cao, *Chem. Lett.*, 2002, 484.
16 (*a*) N. Massayuki and A. J. Yoshihiro, *J. Non-Cryst. Solids*, 1996, **197**, 73; (*b*) X. L. Wang, Y. Q. Guo, Y. G. Li, E. B. Wang, C. W. Hu and N. H. Hu, *Inorg. Chem.*, 2003, **42**, 4135.
17 O. Kahn, *Molecular Magnetism*, VCH, Weinheim, 1993.

This journal is © The Royal Society of Chemistry 2008